Journal of Peptide Science
J. Pept. Sci. 2007; **13**: 451–457
Published online 8 June 2007 in Wiley InterScience (www.interscience.wiley.com). DOI: 10.1002/psc.866

JOURNAL OF PEPTIDE SCIENCE

Imaging of protein layers with an optical microscope for the characterization of peptide microarrays

VIANNEY SOUPLET, RÉMI DESMET and OLEG MELNYK*

UMR CNRS 8161 – CNRS/Université de Lille 1 et 2/Institut Pasteur de Lille, Institut de Biologie de Lille, 59021 Lille, France

Received 13 February 2007; Accepted 19 February 2007

Abstract: Solid-phase assays play a crucial role today in biological studies. These assays are based on the immobilization of probe molecules on a surface, which are able to capture specifically soluble receptors. In particular, peptide microarrays have emerged as powerful tools in a variety of applications. In this context, optical techniques that allow imaging of nanometer-thick biomolecular films, and thereby the characterization of microarrays, are of great interest. For this purpose, we used a recently disclosed wide-field optical imaging technique of surface nanostructures called Sarfus, which is based on the use of a standard optical microscope and antireflection substrates. We demonstrate here that this technique allows the imaging of the protein layers that result from the specific capture of antibodies by arrayed peptide probes with a spatial resolution of 0.45 μm. The relationship between the thickness of the antibody layer and peptide or antibody concentration was examined. Copyright © 2007 European Peptide Society and John Wiley & Sons, Ltd.

Keywords: imaging; peptide; antibody; protein layer; microarray; Sarfus technique

INTRODUCTION

Peptide microarrays are analytical devices that permit the detection of a large number of analytes in biological samples [1–3]. They are composed of a planar solid substrate covered by an array of peptide probe molecules. The probes are immobilized on the surface at well-defined positions, typically as spots with a diameter usually between 50 and 250 μm. The detection of the captured molecules can be done using mainly optical [4], electrical [5], or mechanical [6] methods. Fluorescence, which is certainly the most frequently used detection technique in this field, usually requires the derivatization of the biological samples or of specific reagents with a fluorescent dye [7]. The diversity of interactions that can be studied using these miniaturized analytical devices has generated many applications such as the serodiagnosis of infectious diseases [8,9], high-throughput cell adhesion assays [3], or the evaluation of protein kinase activity [10]. In this context, methods allowing the imaging of nanometer-thick films are of great interest for the characterization and optimization of microarray fabrication. Such quality control can be carried out using ellipsometry [11–15]. Here we demonstrate that a recently disclosed wide-field optical imaging technique of surface nanostructures called *Sarfus* allows the rapid imaging of protein films formed by the specific capture of antibodies by arrayed peptide probes, and thereby can be used for the characterization of peptide microarrays.

The Sarfus technique is based on the use of a standard optical microscope and antireflection substrates. Optical microscopy is a well-established, low-cost, and widely used technique for probing surface structures and studying thin-film properties. The image contrast in reflection microscopy can be increased by using reflected differential interference contrast (DIC) [16]. A way to further increase the image contrast is to use a substrate that reflects light only if the surface is covered by a thin film. However, such antireflecting properties have been observed only with normal incidence of light and therefore could not be combined with optical microscopes for contrast enhancement. Ausserré and Valignat [17,18] have recently described a novel substrate that has antireflecting properties when working at non-normal incidence with polarized light. As a consequence, these substrates (called Surfs) are compatible with the optical microscope. The antireflecting property is lost as soon as some material is present on the surface. As an example, we have recently reported the use of the Sarfus technique for the characterization of micropatterns of silica nanoparticles (dia. 27 nm) on a polycarbonate substrate [19].

In this work, we have evaluated for the first time the capability of the Sarfus technique to image and measure the biomolecular films that are formed on the surface from the specific binding of the immobilized peptide probes by soluble targets. Well-known tag peptides derived from influenza hemagglutinin (HA) [20] or *myc* protein (*myc*) [21] and their corresponding murine antibodies were used in this study. The tag peptides were microarrayed either on amine-modified Surf substrates (**Sa** substrates) or amine-modified microscope glass slides (**Sb** substrates)

*Correspondence to: O. Melnyk, UMR CNRS 8161 – CNRS/Université de Lille 1 et 2/Institut Pasteur de Lille, Institut de Biologie de Lille, 1 rue du Pr Calmette, 59021 Lille, France; e-mail: oleg.melnyk@ibl.fr

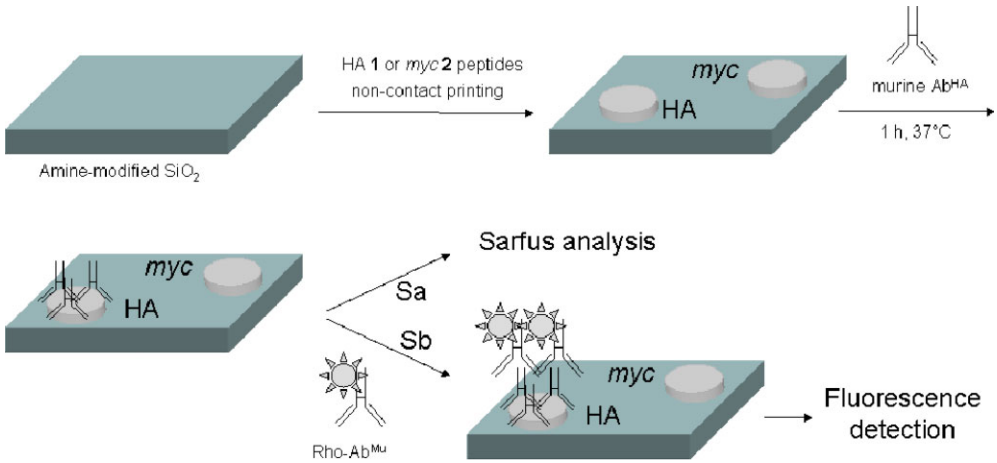

Figure 1 HA **1** and *myc* **2** peptide printing on amine-modified **Sa** or **Sb** surfaces using a noncontact microarrayer and incubated with murine anti-HA or anti-*myc* antibodies. **Sa** microarrays were analyzed directly with an optical microscope after the incubation with the antibodies. **Sb** surfaces were further incubated with goat anti-murine IgG antibodies labeled with tetramethylrhodamine for fluorescence detection. The **Sb** microarrays were analyzed at 532 nm using a standard fluorescence microarray scanner.

using a noncontact piezoelectric microarrayer. The surfaces were incubated with different concentrations of anti-HA or anti-*myc* antibodies. **Sa** substrates were directly observed with an optical microscope and the influence of peptide or antibody concentration on the microspot thickness was examined. **Sb** substrates were used as a control for specificity. **Sb** substrates were incubated with anti-HA or anti-*myc* antibodies and tetramethylrhodamine-labeled goat anti-murine antibodies, respectively, to be analyzed with a standard fluorescence microarray scanner.

RESULTS AND DISCUSSION

HA **1** (32 amino acids) and *myc* **2** (36 amino acids) peptides were synthesized on the solid phase using standard Fmoc/tert-butyl chemistry [22] and purified by RP-HPLC. The peptides were dissolved at different concentrations from 0.5 to 100 μM (six concentrations) in a sodium acetate buffer and printed on amine-modified **Sa** or **Sb** surfaces using a noncontact piezoelectric arrayer (three drops, 1 nl overall). Amine-modified silica surfaces are good substrates for peptide or protein immobilization by physisorption [23,24], and therefore are often used for the preparation of peptide or protein microarrays [8,25,26]. The variation of the microspot thickness due to the capture of antibodies from the aqueous medium by the immobilized peptides was not expected to exceed few nanometers [27–30]. Consequently, the **Sa,b** substrates were covered by an amine layer of regular thickness and low roughness. This was achieved by treating silica substrates with H_2SO_4/H_2O_2 and 3-aminopropyltrimethoxysilane in 10% aqueous MeOH successively as described elsewhere [25]. This procedure yields a regular 2-nm amine layer that displayed an rms roughness of about 1 nm as determined by atomic force microscopy (AFM).

The **Sa,b** microarrays were incubated with commercially available anti-HA or anti-*myc* murine antibodies in the presence of Tween 20 and 2% bovine serum albumin (BSA), and washed successively with PBS, water, and ethanol (Figure 1). **Sa** substrates were imaged using the Sarfus technique before and after incubations with the antibodies. **Sb** microarrays prepared on microscope glass slides required a second incubation step with goat anti-murine IgG antibodies labeled with tetramethylrhodamine to reveal the primary murine antibodies captured by the immobilized peptide. Fluorescence detection was performed at 532 nm using a standard confocal microarray scanner.

Figure 2 illustrates the method used to quantify the thickness of the microspots. A typical Sarfus image of a microspot of peptide HA **1** (100 μM) incubated with anti-HA antibodies (10 μg/ml) at 0.45 μm lateral resolution is shown in Figure 2(A). The size of the image is 365 × 284 μm. The thickness of the layers present on the substrate can be visualized using a false-color scale as shown in Figure 2(B). Correspondence between the layer thickness and color was obtained using a stair-like sample built on a Surf substrate. The preparation and properties of this sample is described in detail elsewhere [17]. The stair is made of seven silica steps whose heights with respect to the oxide layer are 2.0, 10.1, 18.3, 22.3, 30.7, 37.6, and 41.4 nm. Observation of this stair sample with the Sarfus technique allows the calibration of the instrument. Figure 2(C) corresponds to a 3D view of the spot. Figure 2(D) gives the thickness of the layer on the substrate along the doted line shown in Figure 2(B), which goes twice through the center of the microspot. The microspot (~250 μm in diameter) appears as a plateau on the surface with a height of about 3 nm with respect to the amine

DOI: 10.1002/psc

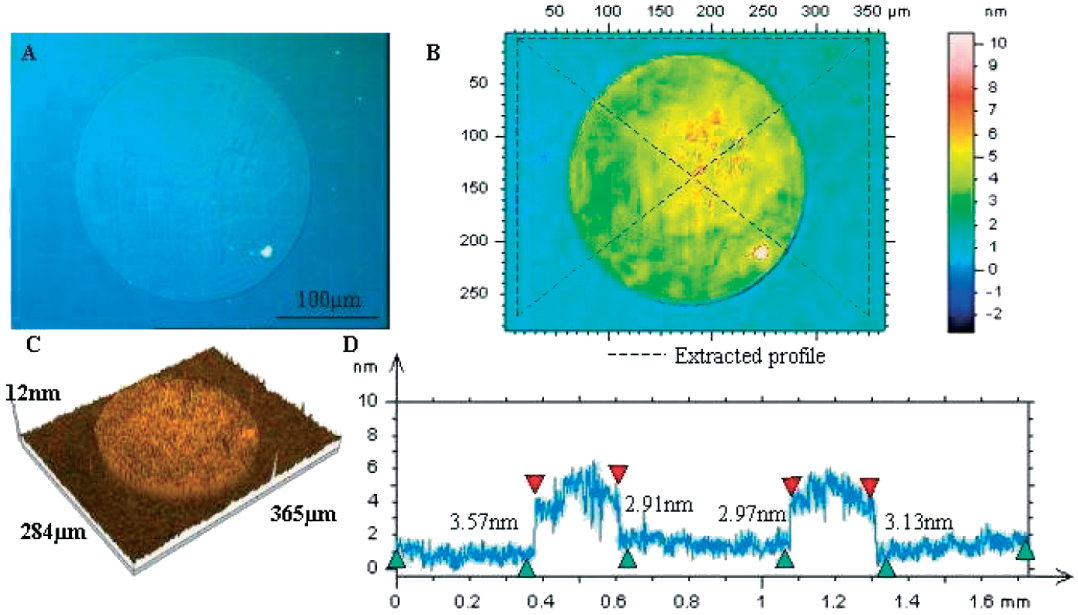

Figure 2 Sarfus image of a microspot of peptide HA **1** printed at 100 µM on a Surf substrate silanized with 3-aminopropyltrimethoxysilane and incubated for 1 h at 37 °C with murine anti-HA antibodies (10 µg/ml in PBS containing 0.05% Tween 20 and 2% BSA). (A) Microscope image at 20× objective magnification. The size of the image is 365 × 284 µm and the lateral resolution 0.45 µm. (B) Same image as in A but using a false-color scale to better visualize the optical thickness of the different layers. (C) Sarfus 3D representation of the microspot. (D) Optical thickness of the layers along the dotted line shown in B (extracted profile). The dotted line goes twice through the center of the microspot and four times through the step at the boundary between the bare substrate and the periphery of the microspot. The mean height of the step is about 3 nm.

substrate. The profile defined by the dotted line in Figure 2(B) allows measurement four times the step at the boundary between the substrate and the microspot as shown by the marks in Figure 2(D). The thickness of the microspot is defined as the mean of these four measurements. Each peptide concentration was printed in triplicate and all the incubations were also performed in triplicate. Thus, the thickness of a microspot is determined by 36 measurements.

Sa microarrays were first analyzed after washing and saturation in the presence of BSA (Figure 3). In this case, the height of the spots was found to be usually negative. For example, the height of peptide HA microspot at 5 µM was −0.15 nm relative to the amine substrate. These results can be explained by a reduced adsorption of BSA on the surface already covered by peptide molecules compared to the amine-modified surface around the peptide microspot. Since the size of peptide molecules (about 4 kD) is significantly smaller than that of BSA (66 kD), differential adsorption of BSA between the peptide microspot and the bare substrate can lead to negative heights. In contrast to the *myc* **2** peptide, the thickness of the HA **1** microspot increased significantly with peptide concentration. This difference could be due to the greater hydrophilicity of the *myc* **2** peptide (15 polar and 9 hydrophobic amino acids) compared to HA **1** peptide (6 polar and 12 hydrophobic amino acids), leading to the partial desorption of the former during the washing step.

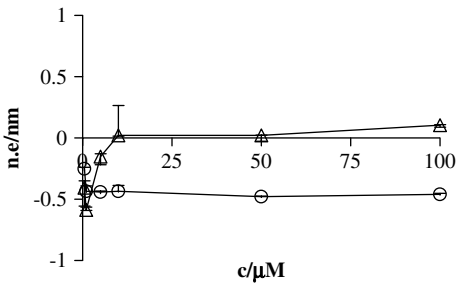

Figure 3 Peptide HA **1** (Δ) and *myc* **2** (○) printed on amine-modified Surf substrates at different concentrations from 0 to 100 µM. **Sa** microarrays were washed with PBS containing 0.05% Tween 20 and 2% of BSA and analyzed using the Sarfus technique. The optical thickness n.e. (nm) relative to the bare substrate is given as a function of peptide concentration. The data correspond to the median and interquartile range for three spots.

We next examined the capture of purified antibodies by the arrayed peptide probes on **Sa** substrates. Figure 4(A) and (C) shows the peptide HA **1** (100 µM) microspot incubated with anti-HA or anti-*myc* antibodies (250 µg/ml in PBS), respectively, at 0.45 µm lateral resolution. Analogously, Figure 4(B) and (D) corresponds to peptide *myc* **2** microspot incubated with anti-HA or anti-*myc* antibodies, respectively. A spot is clearly visible when a peptide was incubated with its specific antibody, i.e. peptide HA **1** with anti-HA antibody (Figure 4(A)) or peptide *myc* **2** with anti-*myc*

DOI: 10.1002/psc

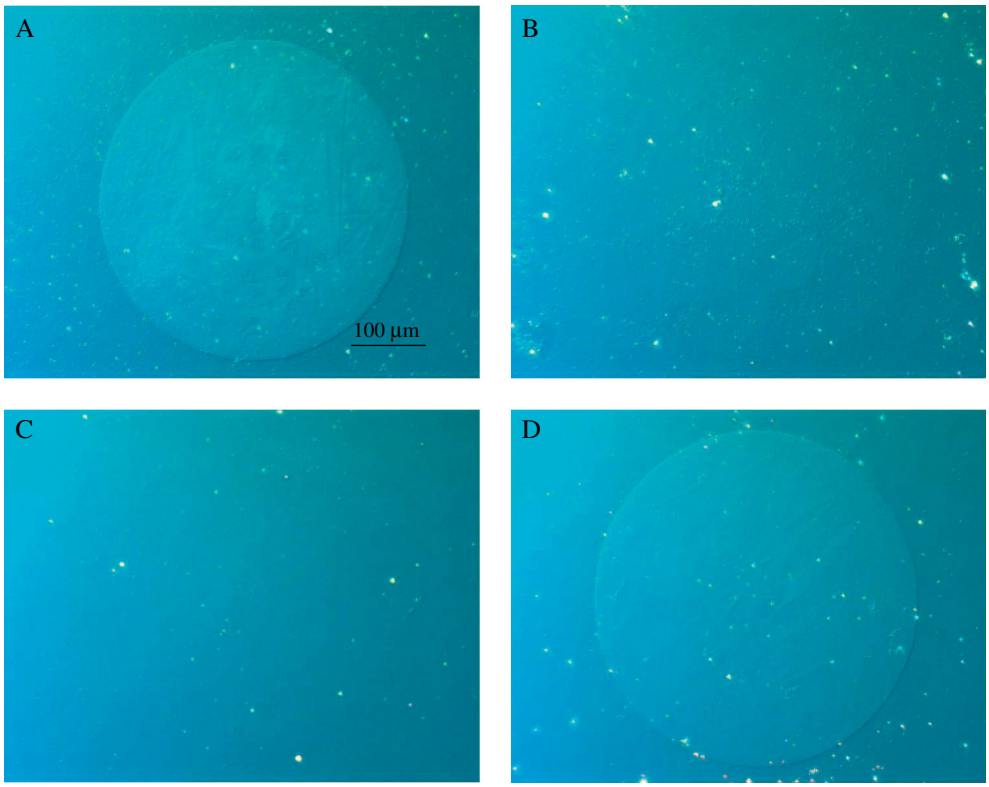

Figure 4 HA **1** and *myc* **2** peptides printed at 100 µM on amine-modified **Sa** substrate using a noncontact arrayer (three drops, ~1 nl). The microarrays were incubated for 1 h at 37 °C with anti-HA (A, B) or anti-*myc* (C, D) antibodies (250 µg/ml) diluted in PBS containing 2% BSA and 0.05% Tween 20. The substrates were imaged using an optical microscope in Sarfus configuration.

antibody (Figure 4(D)), whereas no significant change could be observed for the HA **1** microspots in the presence of anti-*myc* antibody (Figure 4(C)) or for the *myc* **2** microspots in the presence of anti-HA antibody (Figure 4(B)). These results demonstrate that the Sarfus technique permits the rapid imaging of the protein layers formed by the specific binding of antibodies to arrayed peptide probes.

We next examined the effect of peptide or anti-HA antibody concentration on the height of the HA **1** or *myc* **2** microspots. The peptides were printed at six different concentrations in triplicate from 0.5 to 100 µM. The anti-HA antibody concentration was varied from 0.01 to 10 µg/ml. Each antibody concentration was tested in triplicate, and the data presented in Figure 5 correspond to the median and interquartile range of the microspot heights with respect to the amine-modified substrate. The spot heights were found to be highly reproducible (Figure 5).

Negative microspot heights were observed for HA **1** peptide printed at 1 µM irrespective of the anti-HA antibody concentration tested (Figure 5). However, the specific binding of anti-HA antibodies (10 µg/ml) to the HA **1** microspots could be detected using **Sb** substrates and fluorescence detection (data not shown). Thus, at 1 µM peptide concentration, the surface density of peptide/antibody complexes is probably not high enough to give a layer thicker than the surrounding BSA layer. The molecular weight of BSA and IgG is 66 and 150 kD, respectively. Because of the difference in size between BSA and IgG, the formation of a dense layer of IgG molecules on a peptide microspot is expected to give positive microspot heights, even though the surface surrounding the microspot is saturated with BSA. This was indeed observed for **HA 1** peptide concentrations above 5 µM. The microspot height of the HA **1** microspots incubated with anti-HA antibody reached a plateau for a peptide concentration above 10 µM irrespective of the concentration of antibody used, a phenomenon that can be attributed to the saturation of the surface by peptide molecules above this concentration. Interestingly, the relationship between the anti-HA antibody concentration and HA **1** (50 µM) microspot height was found to be linear (Figure 5, $r^2 = 0.98$).

The altitude of the peptide *myc* **2** microspots is also presented in Figure 5. In contrast to HA **1**, the heights of the *myc* **2** microspots in the presence of anti-HA antibodies at 10 µg/ml were not significantly different from those obtained after washing with BSA/Tween 20, demonstrating that the increase in optical height observed for HA **1** microspots was due to the specific capture of anti-HA antibodies by the immobilized HA **1** peptide.

Sb microarrays combined with fluorescence detection confirmed the specificity of the antibody capture for all

DOI: 10.1002/psc

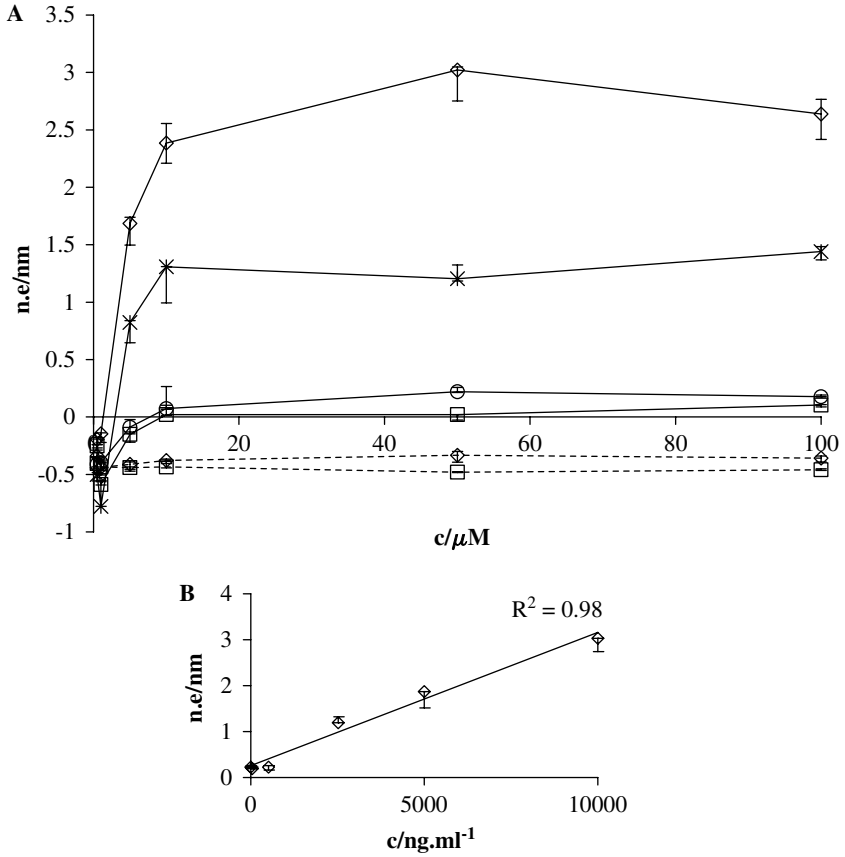

Figure 5 Effect of anti-HA antibody and peptide concentration (HA **1** or *myc* **2**) on the height of the microspots. The n.e. values correspond to the difference between the optical heights of the spots and of the layer between the spots. (A) Peptide HA **1**: continuous line, peptide *myc* **2**: dotted line. Anti-HA antibody: (◊) 10 μg/ml, 2.5 μg/ml (×), 0.001 μg/ml (○), none (□). (B) Relationship between peptide HA **1** microspot height and anti-HA antibody concentration (HA **1** : 50 μM). The data correspond to the median and interquartile range for three microarrays (spots in triplicate).

the peptide or antibody concentrations tested. Figure 6 compares the height of peptide HA **1** microspot printed at 50 μM (**Sa** substrate) and the fluorescence signal of the microspots obtained using the **Sb** substrate. The error in the layer thickness is significantly lower than that in the fluorescence signal, especially for the highest concentrations tested. The microspot fluorescence was found to decrease at high antibody concentrations. However, the height of peptide HA **1** microspot increased even for the highest antibody concentration tested, suggesting that the decrease of microspot fluorescence is probably due to the self-quenching of the rhodamine dye.

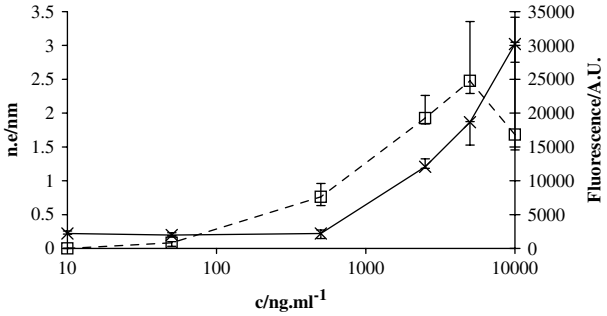

Figure 6 Comparison between Sarfus detection (**Sa**, ×) and fluorescence detection (**Sb**, □) at 532 nm using a standard microarray scanner. Peptide HA **1** (50 μM) was incubated with different concentrations of anti-HA antibodies from 10 to 10 000 ng/ml in PBS containing 0.05% of Tween 20 and 2% BSA. The data correspond to the median and interquartile range for three microarrays (spots in triplicate).

CONCLUSIONS

We have demonstrated that the Sarfus detection technique, based on the use of a microscope equipped with cross-polarizers and Surfs as contrast-enhancing substrates, allows rapid imaging at 0.45 μm resolution of a protein layer formed by the specific binding of antibodies to arrayed peptide probes. The relationship between the layer thickness and antibody concentration was found to be linear. This novel technique, which allows the rapid label-free and wide-field optical imaging of protein layers, can be used for the characterization of polypeptide microarrays as described in this work and, more generally, should be of great interest for those

DOI: 10.1002/psc

interested in the interaction of peptides or proteins with surfaces.

MATERIALS AND METHODS

Surface Fonctionalization

Standard Surfs (SiO_2 surface) were purchased from Nanolane (France). Surfs and microscope glass slides were cleaned using a freshly prepared piranha solution (H_2SO_4/H_2O_2, 1/1 by vol, 1 h). The substrates were washed with water (5 × 3 min) and methanol (3 min) and then treated for 30 min under sonication with 3% 3-aminopropyltrimethoxysilane in 5% aqueous methanol/water solution. The supports were then washed successively with methanol, water (twice), and methanol, and finally annealed for 15 min at 110 °C.

Peptide Synthesis

The sequence of the HA **1**, H-SGYPYDVPDYAGYPYDVPDYA GYPYDVPDYAS-NH_2, is derived from HA, a surface glycoprotein required for infectivity of the human influenza virus. The sequence of the *myc* **2**, H-SEQKLISEEDLNGEQKLISEEDLNA EQKLISEEDLG-NH_2, is derived from the human c-*myc* protein. The peptides were synthetised in an automated peptide synthesizer (Pioneer, Perseptive Biosystems Inc., MA, USA) using the standard Fmoc/*tert*-butyl strategy.

Synthesis of peptides was performed on a 0.1 mmol scale on a Rink Amide resin (Fmoc-PAL-PEG-PS, Perseptive Biosystems, MA, USA). Following peptide elongation, the peptide was deprotected and cleaved during 2 h at room temperature using TFA/water/triisopropylsilane (9.5/250/250 µl). The peptide was precipitated in diethyl ether/*n*-heptane, 1/1 v/v, and then purified by RP-HPLC on a 120 Å 5 µm C18 Nucleosil column using a linear water/acetonitrile gradient containing 0.05% TFA by vol (6 ml/min, detection 230 nm) to give 54 mg of HA **1** and 15 mg of *myc* **2** after lyophilization.

HA **1**: RP-HPLC purity: 92% (C18 Nucleosil, 0-80% acetonitrile containing 0.05% TFA in 60 min, 1 ml/min, detection at 215 nm, 50 °C). Capillary electrophoresis purity: >95% (5 kV, phosphate buffer). MALDI-TOF: $[M + H]^+$ calcd monoisotopic: 3748.6; found: 3748.6.

myc **2**: RP-HPLC purity: 89% (C18 Nucleosil, 0–80% acetonitrile containing 0.05% TFA in 60 min, 1 ml/min, detection at 215 nm, 50 °C). MALDI-TOF: $[M + H]^+$ calcd 4074.41; found: 4074.1.

Printing of the Microarrays

Peptides were dissolved at 0.1 mM, 0.05 mM, 0.01 mM, 10 µM, 5 µM, 1 µM and 0.5 µM in 0.1 M pH 5.5 sodium acetate buffer and printed in triplicate (three drops of 300 pl, 1 nl overall) on amine-modified **Sa** or **Sb** substrates using a Perkin-Elmer BioChip Arrayer 1 (Perkin-Elmer, Wellesley, MA, USA). The microarrays were stored at room temperature in a closed box under nitrogen until use.

Incubations

The experiments were performed in triplicate.

PBS-A is a 0.01 M phosphate buffered saline pH 7.2 containing 0.05% of Tween 20. PBS-B was prepared by adding 2% w/v of BSA to PBS-A.

The surfaces were saturated for 5 min at 37 °C with PBS-B. After three washings with PBS-A, the microarrays were incubated 1 h at 37 °C and under coverglass with murine anti-HA (120 µl, monoclonal antiboby HA.11, Eurogentec, Belgium) or anti-*myc* antibodies (120 µl, monoclonal anti-*myc* antibody, Invitrogen, CA, USA) diluted from 1/100 to 1/500 000 in PBS-B. **Sa** substrates were washed three times with PBS-A, distilled water and absolute ethanol and dried in air. **Sb** substrates were washed three times with PBS-A and incubated for 1 h at 37 °C with tetramethylrhodamine-conjugated goat antibodies against murine IgG (1/100 in PBS-B). The slides were then washed three times in PBS-A, distilled water, and absolute ethanol and dried in air.

Sarfus Analysis

Optical observations on Standard Surfs were carried out using a Leica DMR-HC reflection optical microscope (Leica Microsystem, Wetzlar, Germany) equipped with cross-polarizers and DIC. Three-dimensional visualization and thickness measurements of the overlayers were performed by comparing colors and intensities in the sample image (Sarfusoft software by Nanolane) with those of a calibration standard made of nanometer-thick silica steps on a Surf (Nanolane, France).

Fluorescence Analysis

The glass slides were scanned with an Affymetrix 418 array scanner (MWG, Santa Clara, California, USA). The scanner sensitivity was fixed at 50% laser power and 70% PMT. The data were analyzed using the Perkin-Elmer ScanArrays Express software (Perkin-Elmer, Wellesley, MA, USA).

Acknowledgments

We would like to thank CNRS, Université de Lille 1 et 2 and Institut Pasteur de Lille for financial support. The microarray facility (Institut de Biologie de Lille) and the Sarfus microscope weres financed by the Région Nord Pas de Calais, the European Community (FEDER) and the Ministère de la Recherche et des Nouvelles Technologies (puces nano-3D and FANSBAMED projects). Finally, we thank ANRT for financial support (grant to V. Souplet). We thank Nicolas Medard and Dominique Ausserré for useful discussions.

REFERENCES

1. Templin MF, Stoll D, Schrenk M, Traub PC, Vohringer CF, Joos TO. Protein microarray technology. *Trends Biotechnol.* 2002; **20**: 160–166.
2. Xu Q, Lam KS. Protein and chemical microarrays-powerful tools for proteomics. *J. Biomed. Biotechnol.* 2003; **2003**: 257–266.
3. Falsey JR, Renil M, Park S, Li S, Lam KS. Peptide and small molecule microarray for high throughput cell adhesion and functional assays. *Bioconjug. Chem.* 2001; **12**: 346–353.

4. Brecht A, Gauglitz G. Optical probes and transducers. *Biosens. Bioelectron.* 1995; **10**: 923–936.
5. Cui Y, Wei Q, Park H, Lieber CM. Nanowire nanosensors for highly sensitive and selective detection of biological and chemical species. *Science* 2001; **293**: 1289–1292.
6. Ilic B, Czaplewski D, Craighead HG, Neuzil P, Campagnolo C, Batt C. Mechanical resonant immunospecific biological detector. *Appl. Phys. Lett.* 2000; **77**: 450–452.
7. Schaferling M, Nagl S. Optical technologies for the read out and quality control of DNA and protein microarrays. *Anal. Bioanal. Chem.* 2006; **385**: 500–517.
8. Mezzasoma L, Bacarese-Hamilton T, Di Cristina M, Rossi R, Bistoni F, Crisanti A. Antigen microarrays for serodiagnosis of infectious diseases. *Clin. Chem.* 2002; **48**: 121–130.
9. Petrik J. Microarray technology: the future of blood testing? *Vox Sang.* 2001; **80**: 1–11.
10. Houseman BT, Huh JH, Kron SJ, Mrksich M. Peptide chips for the quantitative evaluation of protein kinase activity. *Nat. Biotechnol.* 2002; **20**: 270–274.
11. Venkatasubbarao S, Beaudry N, Zhao Y, Chipman R. Evanescent-imaging-ellipsometry-based microarray reader. *J. Biomed. Opt.* 2006; **11**: 014028.
12. Jin G, Tengvall P, Lundstrom I, Arwin HA. Biosensor concept based on imaging ellipsometry for visualization of biomolecular interactions. *Anal. Biochem.* 1995; **232**: 69–72.
13. Arwin H, Poksinski M, Johansen K. Total internal reflection ellipsometry: principles and applications. *Appl. Opt.* 2004; **43**: 3028–3036.
14. Bakker JW, Arwin H, Lundstrom I, Filippini D. Computer screen photoassisted off-null ellipsometry. *Appl. Opt.* 2006; **45**: 7795–7799.
15. Wang G, Arwin H, Jansson R. Optimization of off-null ellipsometry in sensor applications. *Appl. Opt.* 2004; **43**: 2000–2005.
16. Murphy D. *Differential Interference Contrast (DIC) Microscopy and Modulation Contrast Microscopy. Fundamentals of Light Microscopy and Digital Imaging.* Wiley-Liss: New York, 2001.
17. Ausserre D, Valignat MP. Wide-field optical imaging of surface nanostructures. *Nano Lett.* 2006; **6**: 1384–1388.
18. Burghardt S, Hirsch A, Medard N, Kachfhe RA, Aussere D, Valignat MP, Gallani JL. Preparation of highly stable organic steps with a fullerene-based molecule. *Langmuir* 2005; **21**: 7540–7544.
19. Carion O, Souplet V, Olivier C, Maillet C, Medard N, El-Mahdi O, Durand JO, Melnyk O. Chemical micropatterning of polycarbonate for site-specific peptide immobilization and biomolecular interactions. *Chembiochem* 2007; **8**: 315–322.
20. Looney DJ, Hayashi S, Nicklas M, Redfield RR, Broder S, Wong-Staal F, Mitsuya H. Differences in the interaction of HIV-1 and HIV-2 with CD4. *J. Acquir. Immune. Defic. Syndr.* 1990; **3**: 649–657.
21. Evan GI, Lewis GK, Ramsay G, Bishop JM. Isolation of monoclonal antibodies specific for human c-myc proto-oncogene product. *Mol. Cell. Biol.* 1985; **5**: 3610–3616.
22. Fields GB, Noble RL. Solid phase peptide synthesis utilizing 9-fluorenylmethoxycarbonyl amino acids. *Int. J. Pept. Protein Res.* 1990; **35**: 161–214.
23. Yeo DS, Panicker RC, Tan LP, Yao SQ. Strategies for immobilization of biomolecules in a microarray. *Comb. Chem. High Throughput Screen.* 2004; **7**: 213–221.
24. Tertykh VA, Yanishpolskii VV. Adsorption and chemisorption of enzymes and other natural macromolecules on silicas. *Surfactant Science Series* 2000; **90**: 523–564.
25. Duburcq X, Olivier C, Desmet R, Halasa M, Carion O, Grandidier B, Heim T, Stievenard D, Auriault C, Melnyk O. Polypeptide semicarbazide glass slide microarrays: characterization and comparison with amine slides in serodetection studies. *Bioconjug. Chem.* 2004; **15**: 317–325.
26. Robinson WH, DiGennaro C, Hueber W, Haab BB, Kamachi M, Dean EJ, Fournel S, Fong D, Genovese MC, de Vegvar HE, Skriner K, Hirschberg DL, Morris RI, Muller S, Pruijn GJ, Van Venrooij WJ, Smolen JS, Brown PO, Steinman L, Utz PJ. Autoantigen microarrays for multiplex characterization of autoantibody responses. *Nat. Med.* 2002; **8**: 295–301.
27. Qian W, Yao D, Xu B, Yu F, Lu Z, Knoll W. Atomic force microscopic studies of site-specific immobilization of antibodies using their carbohydrate residues. *Langmuir* 1999; **11**: 1399–1401.
28. Harris LJ, Larson SB, Hasel KW, Day J, Greenwood A, McPherson A. The three-dimensional structure of an intact monoclonal antibody for canine lymphoma. *Nature* 1992; **360**: 369–372.
29. Wrigley NG, Brown EB, Daniels RS, Douglas AR, Skehel JJ, Wiley DC. Electron microscopy of influenza haemagglutinin-monoclonal antibody complexes. *Virology* 1983; **131**: 308–314.
30. Wrigley NG, Brown EB, Skehel JJ. Electron microscopic evidence for the axial rotation and inter-domain flexibility of the Fab regions of immunoglobulin G. *J. Mol. Biol.* 1983; **169**: 771–774.